Dalton Transactions

Dynamic Article Links

Cite this: *Dalton Trans.*, 2011, **40**, 1332

www.rsc.org/dalton

PAPER

Identification of geometrical isomers using vibrational circular dichroism spectroscopy: a series of mixed-ligand complexes of diamagnetic Co(III) ions†

Hisako Sato,*[a] Hidemitsu Uno[a] and Haruyuki Nakano[b]

Received 6th October 2010, Accepted 23rd November 2010
DOI: 10.1039/c0dt01342k

Vibrational circular dichroism (VCD) spectra were measured on the chloroform solutions of a series of mixed-ligand diamagnetic Co(III) complexes, $[Co(tfac)_n(acac)_{3-n}]$ (n = 0–3, tfac = 1,1,1-trifluoro-2,4-pentanedionato; acac = acetylacetonato). Distinct differences were observed in the VCD spectra among the geometrical isomers of the same ligand composition. Such differentiation was hardly possible by their infra-red spectra alone. The structural identification of these isomers was performed in conjunction with DFT calculations.

Introduction

Vibrational circular dichroism (VCD) is the extension of electronic circular dichroism (ECD) into the infrared and near-infrared regions of the spectrum where vibrational transitions occur in the ground electronic state of a molecule.[1–4] The method measures the differential absorption of left *versus* right circularly polarized IR radiation by a molecular vibrational transition. One of the advantages of VCD over ECD is the large amount of information concerning the $3N-6$ normal modes of the molecule, where N is the number of atoms in the molecule.

In recent years, the application of the VCD and Raman optical activity methods has been extended to the scope of metal complexes.[5–22] The absolute configuration or conformation of a coordinated ligand in a solution is analyzed by comparing calculated and experimental spectra.[10] The fine structure in the vibrational energy levels, as well as the presence of cooperative dynamics among ligands, are revealed by these spectroscopic methods.[18] For a systematically varied series of Ru(III) metal complexes, our previous work demonstrated how the VCD spectra were dependent on the fundamental coordination character of the complexes, *e. g.* ΔΛ configuration, ligand chirality and geometrical isomerism.[19] There existed some difficulty, however, in applying VCD calculation to open-shell Ru(III) metal complexes.

Motivated by the above background, the present work includes experimental and theoretical studies on the VCD spectra of a series of mixed-ligand diamagnetic Co(III) complexes. The Co(III) complexes were chosen because calculations based on the magnetic field perturbation (MFP) theory are thought to provide more reliable results for diamagnetic complexes than for paramagnetic ones.[2] Thus the results would show how the theory can be applied to the study of the structures of metal complexes. For these purposes, a mixed-ligand Co(III) complex with acetylacetonato (denoted by acac) and 1,1,1-trifluoro-2,4-pentanedionato) (denoted by tfac) ligands was chosen.[21] Achiral ligands were used to make the situation more simple. Fourteen kinds of Co(III) complexes represented by the formula, $[Co(tfac)_n(acac)_{3-n}]$ (n = 0–3), were synthesized and separated into pure enantiomers.

Results

Separation and identification of isomers of $[Co(tfac)_n(acac)_{3-n}]$ (n = 0–3) (Scheme 1)

A crude mixture of $[Co(tfac)_n(acac)_{3-n}]$ (n = 0–3) was obtained by previously reported procedures.[21] The separation if the mono(tfac) (n = 1), bis(tfac) (n = 2) and tris(tfac) (n = 3) complexes was performed by eluting the crude product on a silica gel column with benzene (Experimental section). The further separation of the bis(tfac) complexes to geometrical isomers was performed by high performance liquid chromatography on a silica gel column with benzene as the eluting solvent. This led to the separation of three kinds of isomers, ***trans-cis***, ***cis-trans*** and ***cis-cis***. The identification of four isomers (**mono**, ***cis-cis***, ***mer*** and ***fac***) was made by ^{1}H NMR. It was determined that the ***fac***-isomer possesses C_3 symmetry, while no such symmetry exists for the ***mer***-isomer. In the case of bis(tfac), both the ***trans-cis*** and ***cis-trans*** isomers have C_2 symmetry so that they could not be not differentiated by their NMR spectra. Thus X-ray crystallographic analyses were performed for ***trans-cis***-$[Co(tfac)_2(acac)]$. The results are shown in

[a]*Department of Chemistry, Graduate School of Science and Engineering, Ehime University, Matsuyama, 790-8577, Japan. E-mail: h-sato@ehime-u.ac.jp; Fax: +81-89-927-9599; Tel: +81-89-927-9599*

[b]*Department of Chemistry, Graduate School of Sciences, Kyusyu University, Fukuoka, 812-8581, Japan*

† Electronic supplementary information (ESI) available: The results of chromatographic resolution of $[Co(tfac)_2(acac)]$, the ^{1}H NMR data of the isomers of $[Co(tfac)_n(acac)_{3-n}]$, chiral chromatographic resolution of $[Co(tfac)_n(acac)_{3-n}]$, the circular dichorism spectra of Δ- or Λ-$[Co(tfac)_n(acac)_{3-n}]$, the values of ε and $\Delta\varepsilon$, the value of ε for IR; Vibrational circular dichroism of calculated Δ-$Co(acac)_3$ and observed $Co(acac)_3$. CCDC reference number 789701. For ESI and crystallographic data in CIF or other electronic format see DOI: 10.1039/c0dt01342k

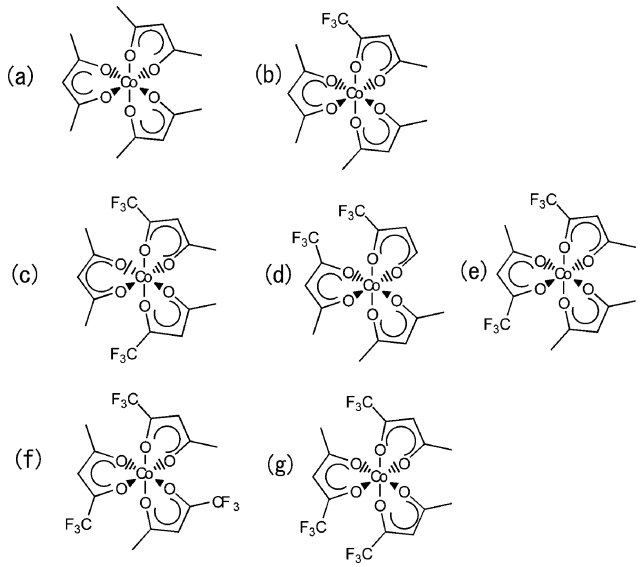

Scheme 1 Geometrical isomers of a series of $[Co(tfac)_n(acac)_{3-n}]$ (n = 0–3) in case of Δ- isomer: (a) $[Co(acac)_3]$, (b) $[Co(tfac)(acac)_2]$, (c) ***trans-cis***-$[Co(tfac)_2(acac)]$, (d) ***cis-trans***-$[Co(tfac)_2(acac)]$, (e) ***cis-cis***-$[Co(tfac)_2(acac)]$, (f) ***fac***-$[Co(tfac)_3]$ and (g) ***mer***-$[Co(tfac)_3]$.

Fig. 1. It was confirmed that two CF_3 groups were located at the *trans*-position. Accordingly the structures of these two types of ***trans-cis*** and ***cis-trans*** isomers were determined.

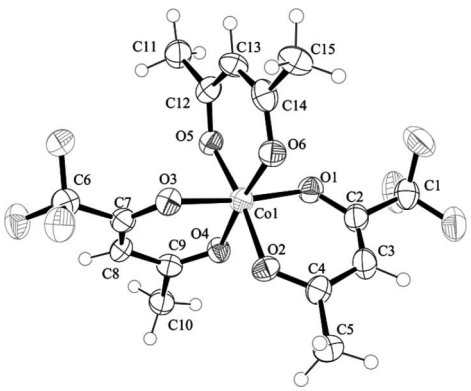

Fig. 1 The ORTEP diagram of Λ-***trans-cis***-$[Co(tfac)_2(acac)]$. The positions of the two CF_3 groups were excluded for clarity.

The further separation of each isomer to its chiral enantiomers was performed by high performance liquid chromatography on a chiral column. A mixture of mono(tfac) complexes was eluted with methanol on the chiral column packed with Δ-$[Ru(phen)_3]^{2+}$/synthetic hectorite.[23] Two peaks (denoted by $\mathbf{1P_1}$ and $\mathbf{1P_2}$, respectively) were obtained. By comparing the CD spectra of these fractions with those of Δ- or Λ-$[Co(acac)_3]$,[24] $\mathbf{1P_1}$ and $\mathbf{1P_2}$ were identified to be Λ- and Δ-$[Co(tfac)(acac)_2]$, respectively. Each of the separated bis(tfac) complexes was eluted on the chiral column with methanol in a similar way. This led to the separation of chiral isomers. They were denoted by ***trans-cis*** ($\mathbf{2P_1}$, $\mathbf{2P_2}$), ***cis-trans*** ($\mathbf{2P_3}$, $\mathbf{2P_4}$) and ***cis-cis*** ($\mathbf{2P_5}$, $\mathbf{2P_6}$). From the CD spectra of these fractions, $\mathbf{2P_1}$, $\mathbf{2P_3}$, and $\mathbf{2P_5}$ were identified to be Λ-isomers, while $\mathbf{2P_2}$, $\mathbf{2P_4}$ and $\mathbf{2P_6}$ were Δ-isomers. When ***fac***-$[Co(tfac)_3]$ was eluted with methanol on the chiral column, two peaks (denoted by $\mathbf{3P_1}$, $\mathbf{3P_2}$, respectively) were obtained. From the CD spectra, $\mathbf{3P_1}$ and $\mathbf{3P_2}$ were identified to be Δ- and Λ-isomers, respectively. When ***mer***-$[Co(tfac)_3]$) was eluted on the same column, a single broad band with a shoulder was obtained. The initial and last parts of the band were collected and named as $\mathbf{3P_3}$ and $\mathbf{3P_4}$. From the CD spectra, $\mathbf{3P_3}$ and $\mathbf{3P_4}$ were identified to be Λ- and Δ-isomers, respectively. The molar extinction coefficients of the UV-vis electronic absorption spectra were determined for their methanol solutions (supporting information†).

Measurements of vibrational circular dichroism spectra of mixed-ligand Co(III) complexes

The VCD spectra of $CDCl_3$ solutions of the separated diastereomers were recorded in the wavenumber region 1000–1800 cm^{-1}. All seven pairs of optical antipodes gave mirror-imaged spectra over the whole wavenumber range, confirming the reliability of the measurements.

Fig. 2 shows the observed VCD (upper) and IR (lower) spectra for the antipodal pair of mono(tfac), Λ-$[Co(tfac)(acac)_2]$/Δ-$[Co(tfac)(acac)_2]$. The solid and dotted lines corresponded to the complexes with Λ and Δ enantiomers, respectively. In order to characterize the spectral features of these isomers, the spectra were divided into the following five regions: Region I (1650–1550 cm^{-1}), Region II (1550–1500 cm^{-1}), Region III (1500–1400 cm^{-1}), Region IV (1400–1350 cm^{-1}) and Region V (1350–1250 cm^{-1}).

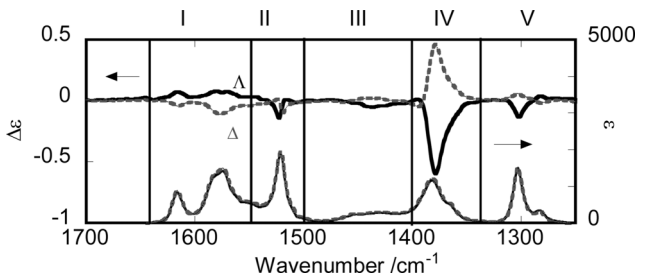

Fig. 2 Observed IR (lower) and VCD (upper) spectra of $[Co(tfac)(acac)_2]$ in $CDCl_3$. Solid and dotted curves correspond to Λ and Δ-enantiomers, respectively.

When the spectra were compared with those of $[Co(acac)_3]$, $[Co(tfac)(acac)_2]$ gave an additional band at the highest wavenumber in Region I due to the replacement of one acac ligand with one tfac ligand.[18] The band was assigned to the C–O stretches intrinsic to the tfac ligands. In Region V, one additional bisignate band appeared around 1320 cm^{-1} for $[Co(tfac)(acac)_2]$. This peak was assigned to the C–C–C bending coupled with the C–CF_3 stretching of tfac ligand.

Fig. 3 (a)–(c) show the observed VCD (upper) and IR (lower) spectra for three antipodal pairs of bis(tfac), ***trans-cis***, ***cis-trans*** and ***cis-cis***-$[Co(tfac)_2(acac)]$, respectively. The solid and dotted lines correspond to the Λ and Δ enantiomers, respectively. In order to characterize the spectral features of these isomers, the whole spectral region was divided into the same five regions as for mono(tfac). One noteworthy aspect was that the VCD spectra differed remarkably between the geometrical isomers, while there was little difference observed in the IR spectra. For example, in Region I, the Δ-***trans-cis*** isomer gave the strong couplet peaks with opposite signs (minus at 1630 cm^{-1} and plus at 1610 cm^{-1}) and the peak with minus sign at 1580 cm^{-1}, while the ***cis-trans*** isomer gave

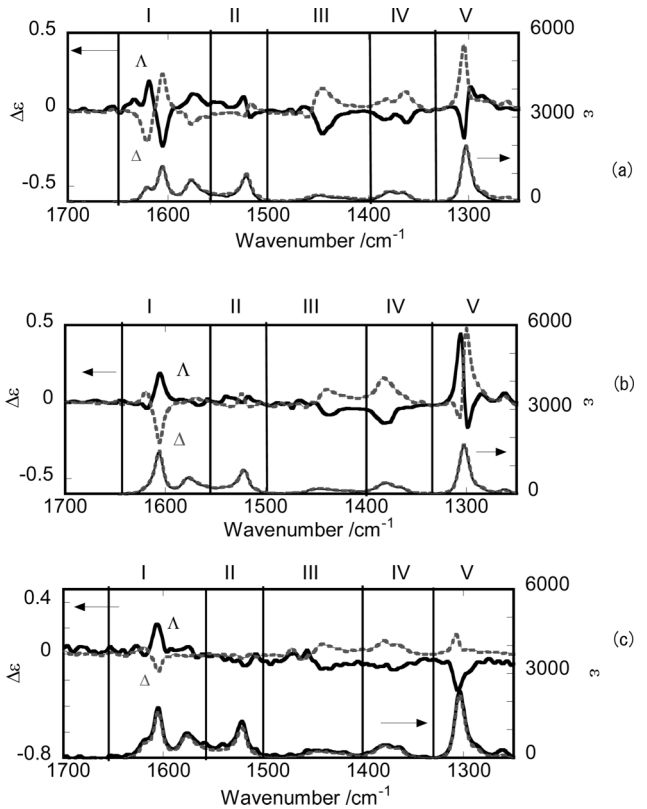

Fig. 3 Observed IR(lower) and VCD (upper) spectra of [Co(tfac)$_2$(acac)] in $CDCl_3$. Solid and dotted curves correspond to Λ and Δ-enantiomers, respectively. (a) ***trans-cis***, (b) ***cis-trans*** and (c) ***cis-cis***-[Co(tfac)$_2$(acac)].

two peaks with small plus, strong minus and small plus peaks in the same region of the VCD spectra. Contrary to this, the Δ-***cis-cis*** isomer gave three peaks with plus, minus and minus signs from the higher to lower wavenumber. Additionally, the Δ-***trans-cis***-isomer gave a split peak around 1300 cm^{-1} in region V with plus and minus signs from the higher to lower wavenumber, while the Δ-***cis-trans*** isomer gave split peaks with the opposite signs. In Regions III, all three isomers displayed a nearly identical broad peak. In Region IV, the ***trans-cis*** isomer gave a doubly split band, while the ***cis-trans*** and ***cis-cis*** isomers gave a broad band.

Fig. 4 (a)–(b) show the observed VCD (upper) and IR (lower) spectra for two antipodal pairs of tris(tfac), ***fac***- and ***mer***-[Co((tfac)$_3$]. The solid and dotted lines corresponded to the Λ and Δ enantiomers, respectively. In order to characterize the spectral features of these isomers, the whole spectral region was divided into the same five regions as for mono(tfac) and bis(tfac). The VCD spectra differed remarkably between these two isomers, while there was little difference observed in the IR spectra over the whole wavenumber region. In Region I, for example, the ***mer***-isomer gave two peaks with nearly equal intensity and the same sign, while the ***fac***-isomer gave two peaks with opposite signs. In other regions they gave nearly the same VCD and IR spectra.

Calculated vibrational circular dichrosim spectra of mixed-ligand Co(III) complexes

Fig. 5 shows the calculated VCD (upper) and IR (lower) spectra of Δ-[Co(tfac)(acac)$_2$]. In order to characterize the spectral features of the isomers, the spectra were divided into the following five

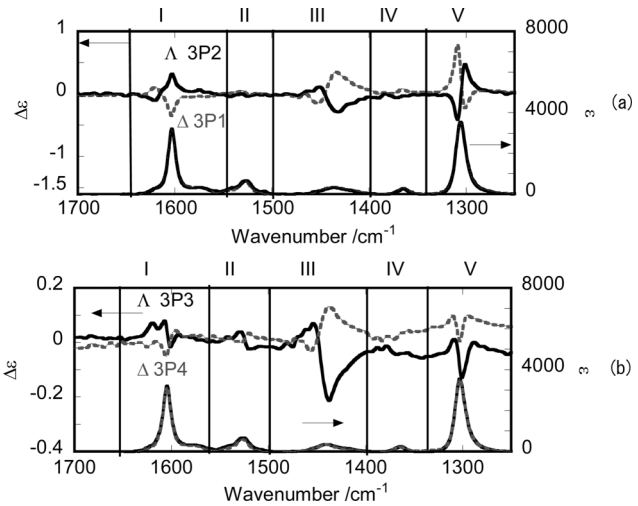

Fig. 4 Observed IR (lower) and VCD (upper) spectra of [Co(tfac)$_3$] in $CDCl_3$. Solid and dotted curves correspond to Λ and Δ-enantiomers, respectively. (a) ***fac*** and (b) ***mer*** isomers are shown.

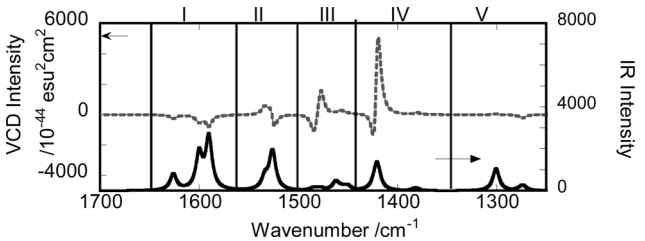

Fig. 5 Calculated IR (lower) and VCD (upper) spectra of Δ-[Co(tfac)(acac)$_2$]. The vertical axes (left) and (right) are the rotational strength and dipole strength (10–40 esu^2 cm^2), respectively. The wavenumber is scaled by 0.97.

regions: Region I (in-phase C–O stretches localized on tfac at higher wavenumber and out-of phase C–O stretches at lower wavenumber on the acac ligands: 1650–1550 cm^{-1}), Region II (C–H bending and C–C–C stretching of tfac or acac ligands: 1550–1500 cm^{-1}), Region III (mostly the C–H_3 of tfac or acac ligands (bending): 1500–1450 cm^{-1}), Region IV (C–C–C bending and C–O stretching, CH_3 (bending) of the tfac ligand or acac ligands: 1450–1350 cm^{-1}) and Region V (C–C–C bending and C–CF_3 stretching of the tfac ligand: 1350–1250 cm^{-1}).

Fig. 6 (a)–(c) show the calculated VCD (upper) and IR (lower) spectra for Δ-***trans-cis***-[Co(tfac)$_2$(acac)], Δ-***cis-trans***- and Δ-***cis-cis***-[Co(tfac)$_2$(acac)], respectively. The spectra were divided into the following five regions: Region I (the in-phase C–O and out-of phase stretches localized on tfac ligands at the lower wavenumber and the C–O stretches localized on the acac ligand: 1650–1550 cm^{-1}), Region II (C–H bending and C–C–C stretching of tfac or acac ligands: 1550–1500 cm^{-1}), Region III (mostly C–H_3(bending) and C–C–C stretching of tfac ligands: 1500–1450 cm^{-1}), Region IV (mostly C–O,C–C–C stretches and CH_3 bending of the acac ligand: 1450–1350 cm^{-1}) and Region V (C–C–C bending and C–CF_3 stretching of tfac ligands: 1350–1250 cm^{-1}).

Fig. 7 (a) and (b) show the calculated VCD (upper) and IR (lower) spectra for Δ-***mer***-[Co(tfac)$_3$] and Δ-***fac***-[Co(tfac)$_3$], respectively. In order to characterize the spectral features of these isomers, the whole spectral region was divided into five regions:

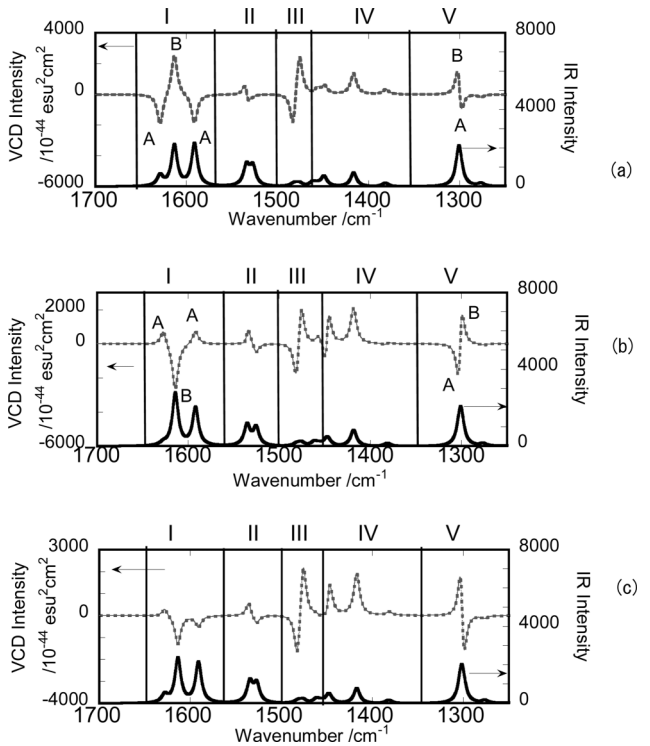

Fig. 6 Calculated IR (lower) and VCD (upper) spectra of Δ-[Co(tfac)$_2$(acac)]. (a) ***trans-cis***, (b) ***cis-trans*** and (c) ***cis-cis***. The ***trans-cis*** and ***cis-trans*** are calculated as having C_2 symmetry. The vertical axes (left) and (right) are the rotational strength and dipole strength (10–40 esu^2 cm^2), respectively. The wavenumber is scaled by 0.97.

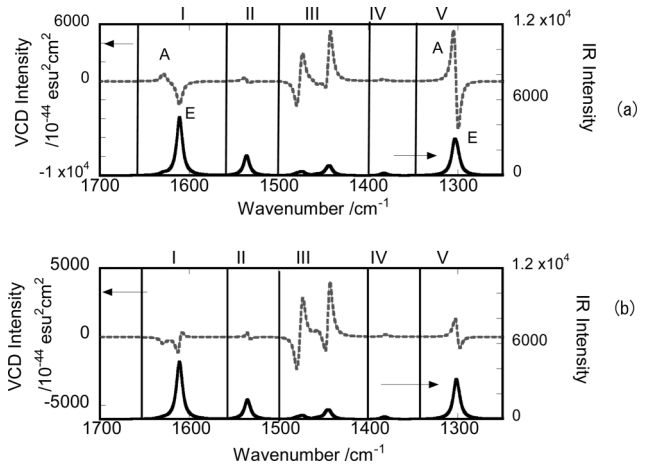

Fig. 7 Calculated IR (lower) and VCD (upper) spectra of (a) Δ-***fac***-and (b) Δ- ***mer***- [Co(tfac)$_3$]. The *fac* isomer is calculated as having C_3 symmetry. The vertical axes (left) and (right) are the rotational strength and dipole strength (10–40 esu^2 cm^2), respectively. The wavenumber is scaled by 0.97.

Region I (the in-phase and out-of phase C–O stretches: 1650–1550 cm^{-1}), Region II (the C–H bending and C–C–C stretching: 1550–1500 cm^{-1}), Region III (mostly CH_3 bending, C–C–C and C–O stretches: 1500–1400 cm^{-1}), Region IV (CH_3 bending: 1400–1350 cm^{-1}) and Region V (C–CF_3 stretching ligand and C–C–C bending: 1350–1250 cm^{-1}). The C–F stretching is assigned to the peaks in the lowest wavenumber region of 1250–1150 cm^{-1} (not shown).

Table 1 The predicted sign of the peaks in the calculated VCD spectra for mixed-ligand Δ-isomers[a,b]

Geometrical isomers	The sign of peaks in Region I	The sign of peaks in Region V
Δ-Co(acac)$_3$[c]	E (–)	No peak predicted
Δ-mono(tfac)	(–) > (–) > (–)	(+) > (–)
Δ-bis(tfac) (***trans-cis***)	A(–) > B(+) > A(–)	B(+) > A(–)
Δ-bis(tfac) (***cis- trans***)	A(+) > B(–) > A(+)	A(–) > B(+)
Δ- bis(tfac) (***cis- cis***)	(+) > (–) > (–)	(+) > (–)
Δ - tris(tfac) (***fac***)	A(+) > E(–: degenerate)	A(+) > E(–:degenerate)
Δ -tris(tfac) (***mer***)	(–) > (–)	(+) > (–)

[a] The peaks are shown in the order of high to low wavenumber [b] A and B denote the Mulliken index for the complexes with C_2 symmetry. A, and E denote the Mulliken index for the complex with C_3 symmetry [c] Supporting information: E denotes the Mulliken index for D_3.†

In all of the above calculated spectra, the complexes give distinct characters. particularly in Regions I and V. The calculated results in these two regions are summarized in Table 1. These predicted features are in good agreement with the observed spectra. Thus the VCD spectra in this region can be used to identify the structures of the geometrical isomers. The results also validated the application of the present theory to diamagnetic Co(III) complexes.

Discussion

This work has presented the first comprehensive VCD spectra for the complete series of tris(chelated) mixed-ligand Co(III) complexes, Δ- or Λ-[Co(tfac)$_n$(acac)$_{3-n}$] (n = 0–3).

Effects of geometrical isomerism

The present results enabled us to compare the VCD spectra among the geometrical isomers of bis(tfac) and tris(tfac) complexes. The difference between these isomers was manifested most remarkably in Region I (C–O stretches) and Region V (mainly C–C–C bending in cooperation with C–CF_3 stretching). In the case of bis(tfac) complexes, for example, two C_2 symmetry isomers gave completely different spectral features; the ***trans-cis*** isomer showed three intense peaks at higher wavenumber, while the ***cis-trans*** isomer showed small and intense peaks. The sign of these peaks is inverted even for the Δ-isomers of the same configuration. It should be noted that both isomers exhibited nearly identical band shapes in their IR spectra. Thus such characterization was only possible with a help of VCD spectra. In the case of the tris(tfac) complexes, two peaks in Region I (in-phase C–O stretching at higher wavenumber) had a different sign, depending on whether they were the ***mer***- or ***fac***-isomers.

Comparison with the theoretical prediction

In the case of mono(tfac) complexes, the theory predicted the sign of peaks in all regions to a satisfactory extent. In the case of bis(tfac) complexes, the theory was successful in predicting the spectral feature of the band in Regions I and V. That is, the C–O band in Region I was predicted to consist of one minus, one plus and one minus peaks for the Δ-***trans-cis*** isomer, while the same band was predicted to consist of one plus, one minus and one plus

peaks or one plus, one minus and one minus peaks for the Δ-***cis-trans*** or Δ-***cis-cis***-isomers, respectively. These predicted features are in accord with the observed spectra. The C–C–C bending band in Region V was predicted to consist of one plus and one minus peaks in Region V for the Δ-***trans-cis*** isomer from higher to lower wavenumber. These features also agree with the observed spectra. The same region was predicted to consist of one minus and one plus peaks in the case of the Δ-***cis-trans*** isomer from higher to lower wavenumber. This is also in accord with the observed spectra. Therefore the geometrical isomers are identified by means of VCD spectra in conjunction with theoretical calculation.

In the case of the ***fac***-isomer, the calculated IR and VCD spectra reproduce well the observed spectra in Regions I and V. For example, the geometrical isomerism on the VCD spectra was predicted correctly by the theory. For the ***mer***-isomer, the calculated IR and VCD in Region I agree well with the observed spectra. VCD is believed to give more reliable results for closed-shell systems than for open-shell systems.[2] Thus the present calculation on diamagnetic Co(III) complexes has provided good examples to validate the application of the magnetic field perturbation (MFP) theory to chiral metal complexes.

Conclusions

This study provided the first comprehensive VCD data for all members of mixed-ligand complexes, Δ- or Λ-[Co(tfac)$_n$(acac)$_{3-n}$] (n = 0–3), in the wavenumber region 1000–1800 cm^{-1}. By comparing the spectra among these molecules, the effects of ΔΛ configuration, and geometrical isomerism were discussed. Additionally, the spectral features (*e.g.* C–O stretchings) were predicted well by the VCD theory based on the magnetic field perturbation (MFP). The result rationalized the approach that geometrical isomers are identified in conjunction with DFT calculations.

Experimental

Materials

[Co(CO$_3$)], (Kanto, Chemical, Co. Inc, Japan) 99% acetylacetonatone (acacH) (Junsei, Chemical. Co., Japan) and 98% 1,1,1-trifluoro-2,4-pentanedionato (denoted by tfacH) (Aldrich), were used as received.

Syntheses and purification of [Co(tfac)$_n$(acac)$_{3-n}$]

The synthesis was carried out according to the reported method.[21] To 0.806 g of CoCO$_3$ (0.68×10^{-2} mol) was added 9.20 ml of tfacH (7.45×10^{-2} mol) and 1.59 ml of acacH (1.53×10^{-2} mol). To this slurry 5.0 ml of 10% H_2O_2 was added dropwise with rapid stirring over a period of 5 min. The mixture was stirred for 0.5 h and the crude product – green crystals – was filtered off, washed with alcohol, and air dried. After separation as described below, the yield was 8.47% (Co(acac)$_3$), 0.12% (Co(tfac)(acac)$_2$), 7.91% (Co(tfac)$_2$(acac)) and 0.44% (Co(tfac)$_3$), respectively. The product was eluted on a silica gel column (30 mm (i.d.) × 200 mm) with benzene. Three bands were separated, leaving unreacted [Co(acac)$_3$] at the top of the column. The first eluted fraction was the mixture of ***mer*** and ***fac*** isomers. The second band was the bis(tfac) isomer. The third band was the mono isomer.

Separation of bis(tfac) isomers

The bis isomers were separated by high performance liquid chromotography on a silica gel column (4 mm × 26 cm, SIL 100A 3 μm) (GL Sciences Inc., Japan) with benzene. The ***trans-cis***, ***cis-trans*** and ***cis-cis*** isomers were separated (supporting information†).

Optical resolution

The separation of diastereomeric isomers of [Co(tfac)$_n$(acac)$_{3-n}$] (n = 0–3) was performed by high performance liquid chromatography on a chiral column (4 mm (i.d.) × 25 cm) packed with an ion-exchange adduct of Δ-[Ru(phen)$_3$]$^{2+}$ (phen = 1,10-phenanthroline) and synthetic hectorite (Ceramosphere RU-1, Shiseido, Japan).[23] Each fraction containing [Co(tfac)$_n$(acac)$_{3-n}$] (n = 0–3) was eluted with methanol at 40 °C (supporting information†). The electronic circular dichrosim (ECD) spectra of the collected fractions are shown in Supporting information.† The determination of Δ, Λ configuration was made by comparing the CD spectra with those of Δ- and Λ-[Co(acac)$_3$].[24]

X-Ray crystallographic analyses

Single crystals of *trans-cis* Λ-[Co(tfac)$_2$(acac)] were prepared by placing an open glass tube containing an ethanol solution of the complex under a hexane atmosphere. Single crystals appeared on the wall of the glass tube. A green needle-shaped crystal with dimension of 0.2 × 0.1 × 0.05 mm^3 was mounted on a 1/4-χ circle diffractometer (AFC8S Mercury CCD, Rigaku Co., Japan). Intensity data were collected with graphite-monochromated Mo Kα radiation (λ = 0.71070 Å) by the following schedule: χ = 54.7°, ϕ = 90°, 2θ = 10°, detector distance = 35 mm, $-80 < \omega < 100$, ω swing width = 0.3°. The intensity data of $6° < 2\theta < 55°$ were processed by application of Lorenz, polarization, and empirical (multi scan) absorption corrections. The crystal data were: $C_{15}H_{15}CoF_6O_6$, orthorhombic, $P2_12_12_1$, a = 8.023(1) Å, b = 11.9970(16) Å, c = 19.429(2) Å, V = 1870.1(4) Å^3, Z = 4, D_{calc} = 1.649 Mg m^{-3}, μ = 1.004 mm^{-1}. The hydrogen atoms were treated as riding. The final R_1 and wR_2 values were 0.0735 and 0.2031, respectively, and the S value was 1.079. The absolute stereochemistry was determined by the abnormal dispersion based on the Flack parameter (–0.07(3)). CCDC No 789701.

Spectroscopic measurements

NMR spectra were measured with a JNM-AL400 (JEOL, Ltd.) in $CDCl_3$. UV-vis spectra were recorded with a U-2810 spectrophotomer (Hitachi, Ltd., Japan). Circular dichroism (CD) spectra were recorded with a J-720 spectropolarimeter (JASCO, Co., Japan). VCD and IR spectra were measured with a PRESTO-S-2007 spectrometer (JASCO, Co., Japan). The machine is the single PEM system, at which the central wavenumber of PEM was set at 1250 cm^{-1}. The calibration was made by use of a quarter wave-retardation and an analyzer. The spectra were recorded on the instrument implemented with the shuttle system. However, we did not used the shuttle system in this work because the signals were large enough for the conventional measurements. A $CDCl_3$ solution of a complex (*ca.* 0.01–0.03 M) was injected into a cell (50–200 μm in optical length) with BaF_2 windows. The signal was accumulated during 10 000 scans (*ca.* 1.5 h) for each complex. The

correction was performed only to subtract the solvent spectra. The resolution of the wavenumber was 4 cm^{-1}. The absorbance of IR spectra was adjusted below 1.0 for the optimal measurements.

Computational details

The IR and VCD spectra of these complexes were theoretically calculated by use of the Gaussian 09 program.[25] VCD intensities were determined by the vibrational–rotational strength and magnetic dipole moments, which were calculated by the magnetic field perturbation (MFP) theory, formulated using magnetic field gauge-invariant atomic orbitals.[2] The calculated intensities were converted to Lorentzian bands with 4 cm^{-1} half-width at half-height. Geometry optimization was performed at the DFT level (B3LYP functional with Stuttgart ECP for Co and 6-31G(d) for other atoms).[26] The electronic configuration of Co(III) ($(t_{2g})^6$) was specified as singlet in the closed-shell system. Two types of ***trans-cis*** and ***cis-trans***-[$Co(tfac)_2$ (acac)] were assumed to have C_2 symmetry. ***fac***-[$Co(tfac)_3$] was assumed to have C_3 symmetry. Others were assumed to have C_1 symmetry. The wavenumber was scaled by 0.97. Thus the peaks in the observed spectrum were assigned on the basis of the animations of molecular vibration with Gauss view 5.08 (Gaussian Inc.).

Acknowledgements

We thank Ms Yuko Hirose and Mr Shota Nakamura (Ehime University) for their synthetic work.

Notes and references

1 J. Hilario, D. Drapcho, R. Curbelo and T. A. Keiderling, *Appl. Spectrosc.*, 2001, **55**, 1435; L. A. Nafie, *Appl. Spectrosc.*, 2000, **54**, 1634; P. Malon and T. A. Keiderling, *Appl. Spectrosc.*, 1996, **50**, 669.
2 J. R. Cheeseman, M. J. Frisch, F. J. Devlin and P. J. Stephens, *Chem. Phys. Lett.*, 1996, **252**, 211; P. J. Stephens, *J. Phys. Chem.*, 1985, **89**, 748; P. J. Stephens and F. J. Devlin, *Chirality*, 2000, **12**, 172; T. B. Freedman, X. Cao, R. K. Dukor and L. A. Nafie, *Chirality*, 2003, **15**, 743; P. Mukhopadhyay, P. Wipf and D. N. Beratan, *Acc. Chem. Res.*, 2009, **42**, 809.
3 S. Abbac, F. Lebon, R. Gangemi, G. Longhi, S. Spizzichino and R. Ruzziconi, *J. Phys. Chem. A*, 2009, **113**, 14851.
4 T. Taniguchi, N. Miura, S.-I. Nishimura and K. Monde, *Mol. Nutr. Food Res.*, 2004, **48**, 246.
5 C. J. Barnet, A. F. Drake, R. Kuroda, S. F. Mason and S. Savage, *Chem. Phys. Lett.*, 1980, **70**, 8.
6 D. A. Young, E. D. Lipp and L. A. Nafie, *J. Am. Chem. Soc.*, 1985, **107**, 6205; D. A. Young, T. B. Freedman, E. D. Lipp and L. A. Nafie, *J. Am. Chem. Soc.*, 1986, **108**, 7255; T. B. Freedman, D. A. Young, M. R. Oboodi and L. A. Nafie, *J. Am. Chem. Soc.*, 1987, **109**, 1551; D. A. Young, T. B. Freedman and L. A. Nafie, *J. Am. Chem. Soc.*, 1987, **109**, 7674.
7 H. Morimoto, I. Kinoshita, M. Mori, Y. Kyogoku and H. Sugeta, *Chem. Lett.*, 1989, **18**, 73; J. Teraoka, N. Yamamoto, Y. Matsumoto, Y. Kyogoku and H. Sugeta, *J. Am. Chem. Soc.*, 1996, **118**, 8875.
8 Y. He, X. Cao, L. A. Nafie and T. B. Freedman, *J. Am. Chem. Soc.*, 2001, **123**, 11320; T. B. Freedman, X. Cao, D. A. Young and L. A. Nafie, *J. Phys. Chem. A*, 2002, **106**, 3560; L. A. Nafie, *J. Phys. Chem. A*, 2004, **108**, 7222; P. R. Lessen, L. Guy, I. Karame, T. Roisnel, N. Vanthuyne, C. Roussel, X. Cao, R. Lombardi, J. Crassous, T. B. Feedman and L. A. Nafie, *Inorg. Chem.*, 2006, **45**, 10230.
9 T. Bas, T. Bürgi, J. Lacour, J. Vachon and J. Weber, *Chirality*, 2005, **17**, S143; M. Bieri, C. Gautier and T. Bürgi, *Phys. Chem. Chem. Phys.*, 2007, **9**, 671; C. Gartier and T. Bürgi, *J. Am. Chem. Soc.*, 2006, **128**, 11079.
10 C. Johannessen and P. W. Thulstrup, *Dalton Trans.*, 2007, 1028.
11 W. Amstrong, F. A. Cotton, A. G. Petrovic, P. L. Polavarapu and M. M. Warnke, *Inorg. Chem.*, 2007, **46**, 1535.
12 J. Stephens, F. J. Devlin, C. Villani, F. Gasparrini and S. L. Mortera, *Inorg. Chim. Acta*, 2008, **361**, 987.
13 P. Nicu, J. Neugebauer and E. J. Baerends, *J. Phys. Chem. A*, 2008, **112**, 6978; V. P. Nicu, J. Autschbach and E. J. Baerends, *Phys. Chem. Chem. Phys.*, 2009, **11**, 1526.
14 G. Jahier, M. Cantuel, N. D. McClenaghan, T. Buffeteau, D. Cavagnat, F. Agbossou, M. Carraro, M. Bonchio and S. Nlate, *Chem.–Eur. J.*, 2009, **15**, 8703.
15 F. De. Montigny, L. Guy, G. Pilet, N. Vanthuyne, C. Roussel, R. Lombardi, T. B. Freedman, L. A. Nafie and J. Crassous, *Chem. Commun.*, 2009, 4841.
16 Z.-B. Han, J.-W. Ji, H.-Y. An, W. Zhang, G.-X. Han, G.-X. Zhang and L.-G. Yang, *Dalton Trans.*, 2009, 9807.
17 V. A. Soioshonok, T. Ono, H. Ueki, N. Vanthuyne, T. S. Balaban, J. Bürch, H. Fliegi, W. Klopper, J.-V. Naubron, T. T. T. Bui, A. F. Drake and C. Roussel, *J. Am. Chem. Soc.*, 2010, **132**, 10477.
18 H. Sato, T. Taniguchi, A. Nakahashi, K. Monde and A. Yamagishi, *Inorg. Chem.*, 2007, **46**, 6755; H. Sato, T. Taniguchi, K. Monde, S.-I. Nishimura and A. Yamagishi, *Chem. Lett.*, 2006, **35**, 364; T. Taniguchi, K. Monde, S.-I. Nishimura, J. Yoshida, H. Sato and A. Yamagishi, *Mol. Cryst. Liq. Cryst.*, 2006, **460**, 107.
19 H. Sato, Y. Mori, Y. Fukuda and A. Yamagishi, *Inorg. Chem.*, 2009, **48**, 4354.
20 H. Sato, D. Shirotani, K. Yamanari and S. Kaizaki, *Inorg. Chem.*, 2010, **49**, 356.
21 R. A. Palmer, R. C. Fay and T. S. Piper, *Inorg. Chem.*, 1964, **3**, 875.
22 S. Luber and M. Reiher, *ChemPhysChem*, 2010, **11**, 1876.
23 A. Yamagishi, *J. Coord. Chem.*, 1987, **16**, 131; J. X. He, H. Sato, Y. Umemura and A. Yamagishi, *J. Phys. Chem. B*, 2005, **109**, 4679.
24 A. F. Drake, J. M. Gould, S. F. Mason, C. Rosin and F. J. Woodley, *Polyhedron*, 1983, **2**, 537.
25 M. J. Frisch, G. W. Trucks, H. B. Schlegel, G. E. Scuseria, M. A. Robb, J. R. Cheeseman, G. Scalmani, V. Barone, B. Mennucci, G. A. Petersson, H. Nakatsuji, M. Caricato, X. Li, H. P. Hratchian, A. F. Izmaylov, J. Bloino, G. Zheng, J. L. Sonnenberg, M. Hada, M. Ehara, K. Toyota, R. Fukuda, J. Hasegawa, M. Ishida, T. Nakajima, Y. Honda, O. Kitao, H. Nakai, T. Vreven, J. A. Montgomery, Jr., J. E. Peralta, F. Ogliaro, M. Bearpark, J. J. Heyd, E. Brothers, K. N. Kudin, V. N. Staroverov, R. Kobayashi, J. Normand, K. Raghavachari, A. Rendell, J. C. Burant, S. S. Iyengar, J. Tomasi, M. Cossi, N. Rega, J. M. Millam, M. Klene, J. E. Knox, J. B. Cross, V. Bakken, C. Adamo, J. Jaramillo, R. Gomperts, R. E. Stratmann, O. Yazyev, A. J. Austin, R. Cammi, C. Pomelli, J. Ochterski, R. L. Martin, K. Morokuma, V. G. Zakrzewski, G. A. Voth, P. Salvador, J. J. Dannenberg, S. Dapprich, A. D. Daniels, O. Farkas, J. B. Foresman, J. V. Ortiz, J. Cioslowski and D. J. Fox, *GAUSSIAN 09 (Revision A.2)*, Gaussian, Inc., Wallingford, CT, 2009.
26 A. Bergner, A. M. Dolg, W. Kuechle, H. Stoll and H. Precuss, *Mol. Phys.*, 1993, **80**, 1431.